



**HAL**  
open science

## Geodynamic significance of the Raspas Metamorphic Complex (SW Ecuador): geochemical and isotopic constraints

Delphine Bosch, Piercarlo Gabriele, Henriette Lapierre, Jean-Louis Malfere, Etienne Jaillard

► **To cite this version:**

Delphine Bosch, Piercarlo Gabriele, Henriette Lapierre, Jean-Louis Malfere, Etienne Jaillard. Geodynamic significance of the Raspas Metamorphic Complex (SW Ecuador): geochemical and isotopic constraints. *Tectonophysics*, 2002, 345 (1-4), pp.83-102. 10.1016/S0040-1951(01)00207-4 . hal-03888527

**HAL Id: hal-03888527**

**<https://hal.science/hal-03888527v1>**

Submitted on 23 Oct 2024

**HAL** is a multi-disciplinary open access archive for the deposit and dissemination of scientific research documents, whether they are published or not. The documents may come from teaching and research institutions in France or abroad, or from public or private research centers.

L'archive ouverte pluridisciplinaire **HAL**, est destinée au dépôt et à la diffusion de documents scientifiques de niveau recherche, publiés ou non, émanant des établissements d'enseignement et de recherche français ou étrangers, des laboratoires publics ou privés.

# Geodynamic significance of the Raspas Metamorphic Complex (SW Ecuador): geochemical and isotopic constraints

Delphine Bosch<sup>a,\*</sup>, Piercarlo Gabriele<sup>b</sup>, Henriette Lapierre<sup>c</sup>, Jean-Louis Malfere<sup>d</sup>,  
Etienne Jaillard<sup>c,e</sup>

<sup>a</sup>Laboratoire de Tectonophysique, UMR-CNRS 5568, CC066, Université de Montpellier II, Place Eugene Bataillon,  
34095 Montpellier, Cedex 05, France

<sup>b</sup>Institut de Minéralogie et Pétrographie, Université de Lausanne, BFSH2, CH-1015, Lausanne, Switzerland

<sup>c</sup>Laboratoire Géodynamique des Chaînes Alpines, UMR-CNRS 5025, Université Joseph Fourier, Maison des Géosciences,  
BP 53, 38041 Grenoble, Cedex, France

<sup>d</sup>Laboratoire de Minéralogie, Géochimie isotopique, Université de Genève, rue des Maraîchers 13, CH-1211 Geneva 4, Switzerland  
<sup>e</sup>IRD, CSSI, 211 rue la Fayette, 75480 Paris, Cedex 09, France

Received 2 May 2000; received in revised form 30 January 2001; accepted 7 February 2001

---

## Abstract

The Raspas Metamorphic Complex of southwestern Ecuador is regarded as the southernmost remnant of oceanic and continental terranes accreted in the latest Jurassic–Early Cretaceous. It consists of variably metamorphosed rock types. (1) Mafic and ultramafic rocks metamorphosed under high-pressure (HP) conditions (eclogite facies) show oceanic plateau affinities with flat REE chondrite-normalized patterns,  $\varepsilon\text{Nd}_{150 \text{ Ma}}$  ranging from +4.6 to 9.8 and initial Pb isotopic ratios intermediate between MORB and OIB. (2) Sedimentary rocks metamorphosed under eclogitic conditions exhibit LREE enriched patterns, strong negative Eu anomalies, Rb, Nb, U, Th, Pb enrichments, low  $\varepsilon\text{Nd}_{150 \text{ Ma}}$  values (from –6.4 to –9.5), and high initial  $^{87}\text{Sr}/^{86}\text{Sr}$  and  $^{206,207,208}\text{Pb}/^{204}\text{Pb}$  isotopic ratios suggesting they were originally sediments derived from the erosion of an old continental crust. (3) Epidote-bearing amphibolites show N-MORB affinities with LREE depleted patterns, LILE, Zr, Hf and Th depletion, high  $\varepsilon\text{Nd}_{150 \text{ Ma}}$  (>+10) and low initial Pb isotopic ratios. The present-day well defined internal structure of the Raspas Metamorphic Complex seems to be inconsistent with the formerly proposed interpretation of a “tectonic mélange”. The association of oceanic plateau rocks and continent-derived sediments both metamorphosed in HP conditions suggests that the thin edge of the oceanic plateau first entered the subduction zone and dragged sediments downward of the accretionary wedge along the Wadatti–Benioff zone. Subsequently, when its thickest part arrived into the subduction zone, the oceanic plateau jammed the subduction processes, due to its high buoyancy. In Ecuador and Colombia, the latest Jurassic–Early Cretaceous suture involves HP oceanic plateau rocks and N-MORB rocks metamorphosed under lower grades, suggesting a composite or polyphase nature for the latest Jurassic–Early Cretaceous accretionary event. © 2002 Elsevier Science B.V. All rights reserved.

*Keywords:* Raspas Metamorphic Complex; Geochemical constraints; Isotopic constraints; Eclogite; Subduction processes

---

## 1. Introduction

The western margin of South America is a classical example of an ocean–continent convergence, which eventually led to the Andean orogeny in Tertiary times. One puzzling problem concerns the significance of the scarce outcrops of high-pressure (HP) metamorphic rocks along the Andean margin. There is no consensus on their tectonic and geodynamic significance and they have been interpreted as related either to subduction, accretion, or collision processes (e.g. Feininger, 1980; Aspden and McCourt, 1986; Bourgois et al., 1987; Aspden et al., 1995; Lucassen et al., 1999).

The western part of northwestern South America (Ecuador and Colombia) is made up of exotic terranes mainly of oceanic origin (Fig. 1), accreted between latest Jurassic and Eocene times (Toussaint and Restrepo, 1994; Litherland et al., 1994; Reynaud et al., 1999; Lapierre et al., 2000; Hughes and Pilatasig, 2001). The eastern boundary of the accreted terranes is marked by the occurrence of tectonic slices of HP metamorphic rocks, which yielded Early Cretaceous cooling ages ( $\approx 132\text{--}110$  Ma) and are thought to represent the suture zone of oceanic terranes accreted during the latest Jurassic–Early Cretaceous times (Feininger, 1982; Aspden and McCourt, 1986; Toussaint and Restrepo, 1994; Litherland et al., 1994, Fig.

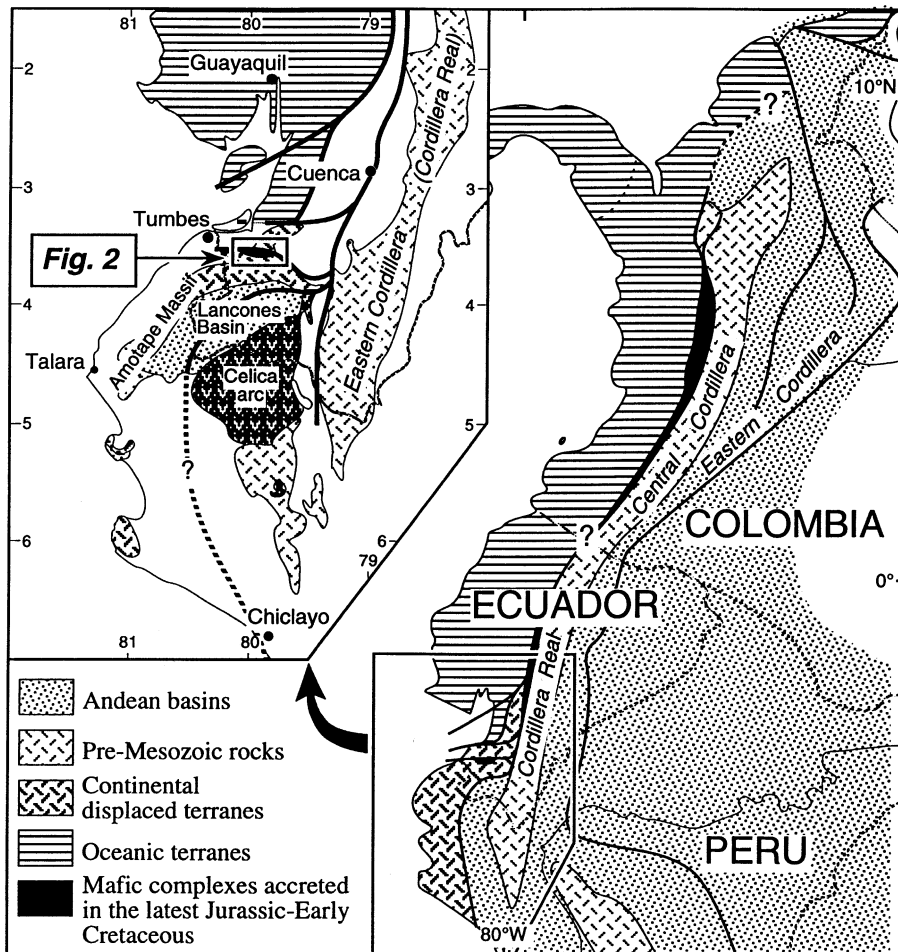


Fig. 1. Structural sketch of northwestern South America showing the exotic terranes accreted in Mesozoic and Cenozoic times and location of the studied area (inset).

1). In Colombia (Kerr et al., 1996, 1997) and SW Ecuador (Arculus et al., 1999; Malfere et al., 1999), a part of the HP metamorphic rocks possesses oceanic plateau affinities.

This paper presents the results of a geochemical study carried out on rocks of the metamorphic Raspas “Ophiolitic” Complex of southwestern Ecuador (Aspden et al., 1995). Since the Raspas outcrops do not show clear evidences of a typical ophiolitic suite and in order to avoid interpretative ambiguities, we shall use in this work the term of “Raspas Metamorphic Complex”. The present study has been undertaken in order to determine the nature and geodynamic significance of the terranes involved in the HP metamorphism, and to test the hypothesis of an accretionary complex.

## 2. Geological setting

In Western Ecuador, the latest Jurassic–Early Cretaceous accretion episode involved both continental and oceanic units (Litherland et al., 1994). The corresponding suture is located at the western edge of the Eastern Cordillera of Ecuador (Pelletier suture, Litherland et al., 1994). It is thought to extend into southwesternmost Ecuador in the El Oro metamorphic complex (Aspden et al., 1995). The latter belongs to the displaced Amotape–Tahuin block (Mourier et al., 1988) and comprises various lithologies and assemblages with ages ranging from Palaeozoic to Cretaceous (Aspden et al., 1995). The El Oro metamorphic complex is crosscut by several E–W trending dextral fault systems that subdivide the El Oro metamorphic complex into various smaller units (Fig. 2).

Among these units, the E–W trending Raspas Metamorphic Complex is bounded to the north and south by the “La Palma–El Guayabo” and the “Tahuin Dam” faults, respectively, which separate the Raspas Metamorphic Complex from rocks belonging to the Andean continental margin (Aspden et al., 1995; Fig. 2). The Raspas Metamorphic Complex consists of greenschists, serpentinitised peridotites, pelitic schists, blueschists and eclogites, first described in detail by Feininger (1980). Phengite K–Ar data ( $132 \pm 5$  Ma; Feininger and Silberman, 1982) points to a lowermost Cretaceous age for the HP metamorphism (Duque, 1993), thus suggesting that it is related

to the latest Jurassic–Early Cretaceous accretion episode (Aspden et al., 1995).

Recent laser Ar/Ar datings have been performed on different samples from the present studied area (Monie et al., in preparation). The analyzed samples include the  $^{97}\text{Ce}1$  eclogite and the  $^{97}\text{Ce}3$  and  $^{97}\text{Ce}5$  metapelites. Ar/Ar ages obtained on both phengite and amphibole range from ca. 122 to 130 Ma. This supports a lower Cretaceous age for the HP event recorded in the Raspas Metamorphic Complex rocks in good agreement with the previous dates (Feininger and Silberman, 1982).

The samples analyzed for geochemistry were collected from the various tectono-metamorphic units defined in the Raspas Metamorphic Complex: the La Chilca, El Toro and Río Panapuli units (Aspden et al., 1995, Fig. 2).

## 3. Lithologies

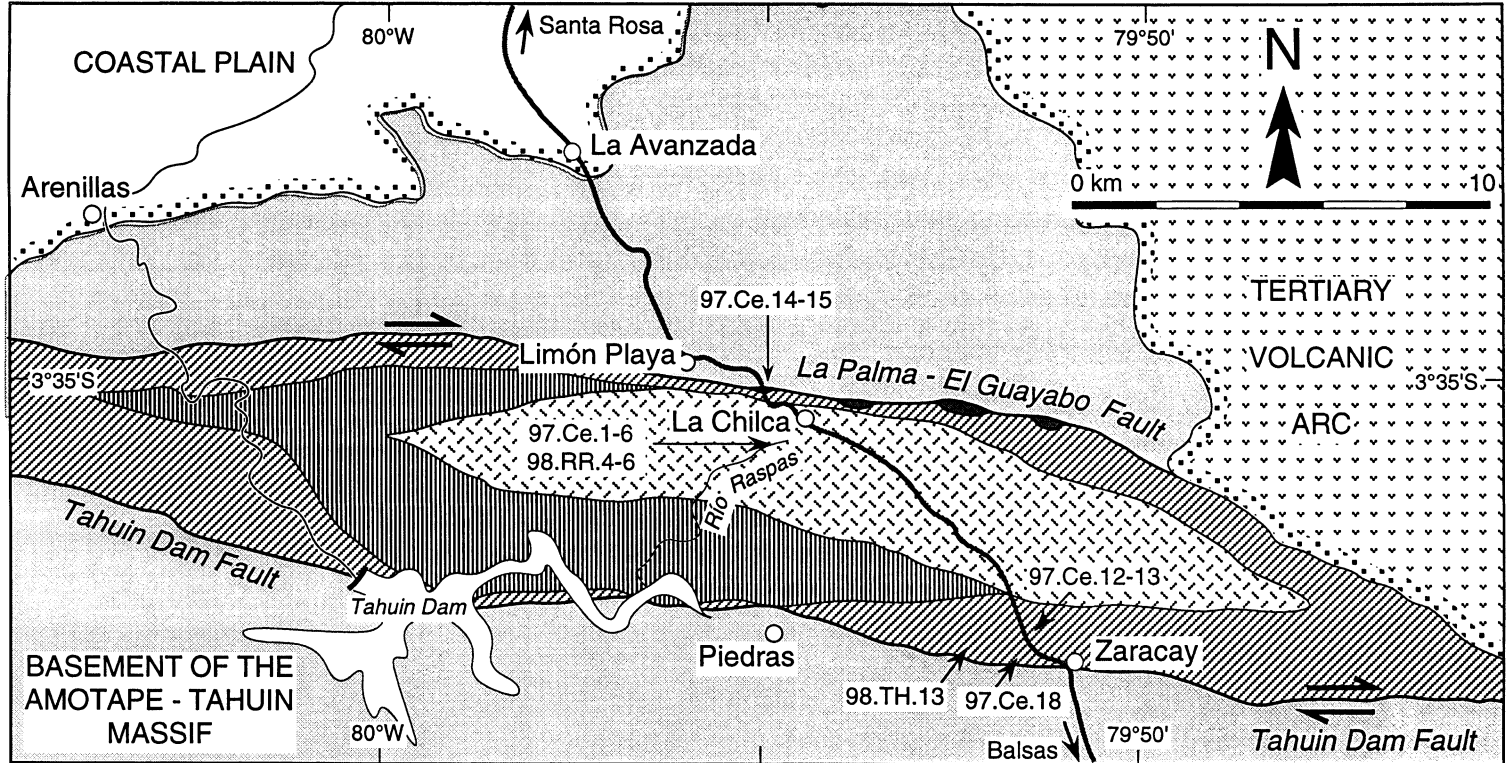
From a petrographic point of view, the analyzed samples can be subdivided into two main groups, namely the metabasites and the metapelites. Table 1 summarizes the paragenesis of the analyzed metamorphic rocks.

### 3.1. The metabasites




The metabasites include eclogites, serpentinitised peridotites and amphibolites of different metamorphic facies. The high-pressure rocks belong to the La Chilca Unit while the amphibolites and greenschists are the main components of the Río Panapuli Unit (Fig. 2).

The eclogites ( $^{97}\text{Ce}1$ , 98RR4, 98RR6) and garnet-amphibolites ( $^{97}\text{Ce}4\text{A}$ ) crop out in the Río Raspas (Fig. 2, UTM-WGS84: 17/620500E-9602100N). The eclogites consist of poikiloblastic garnet, quartz, omphacite, epidote, amphibole (barroisite)  $\pm$  phengite. Their contents in phengite and quartz vary significantly from one facies to another. Garnet commonly includes quartz, rutile and epidote. Zones rich in amphibole or omphacite can lead to a strongly layered texture. The garnet-amphibolites are associated with the eclogites and are characterized by the occurrence of blue-green amphibole.

According to Aspden et al. (1995), the serpentinitised peridotites pinched within the La Palma–El Guayabo



Raspas "Ophiolitic" Complex

-  Río Panupalí unit : metabasites and micaschists
-  El Toro unit : serpentinised peridotites
-  La Chilca unit : metapelites and eclogites

Continental basement units




-  Migmatites, metabasalts, metagabbros, schists, granitoids.
-  Unconformable contacts
-  Main faults

Fig. 2. Structural sketch of the El Oro Metamorphic complex (adapted from Aspden et al., 1995) and location of the studied samples.

Table 1

## Mineral assemblages of the studied metabasites

Sample	97Ce1 [eclogite]	98RR4 [eclogite]	98RR6 [eclogite]	97Ce4A [Grt amphibolite]	97Ce13 [amphibolite (metagabbro)]	97Ce18 [Ep-bearing amphibolite]	98TH13 [Ep-bearing amphibolite]	97Ce12 [Ep-bearing amphibolite]	97Ce14 [serpentinised peridotite]	97Ce15 [serpentinised peridotite]
Qtz	×	×	×	×	×	×	×	×		
Ms		×	×							
Grt	×	×	×	×						
Omp	×	×	×							
Hbl				×	×					
Act						×	×	×		
Tr								×	×	×
Bar	×	×	×							
Ol									×	×
Srp									×	×
Czo	×	×	×	×						
Ep						×	×	×		
Chl				×	×	×	×		×	×
Ab				×		×	×	×		
Pl					×					
Rt	×	×	×	×	×					
Ttn	×	×	×	×		×	×	×		
Cal/Dol					×				×	×
Opaques	×	×	×	×				×	×	×
Met. Facies	eclogite	eclogite	eclogite	epidote- amphibolite	amphibolite	greenschist	greenschist	greenschist	amphibolite	amphibolite

## Mineral assemblages of the studied metapelites

Sample	97Ce2 [metapelite]	97Ce3 [metapelite]	97Ce4 [metapelite]	97Ce5 [metapelite]	97Ce6 [metapelite]
Qtz	×	×	×	×	×
Ms	×	×	×	×	×
Grt	×	×	×	×	×
Cld			×	×	×
Chl	×	×			
Ky				×	×
Rt	×	×	×	×	×
Gr	×	×	×	×	×
Opaques	×		×	×	×
Met Facies	eclogite	eclogite	eclogite	eclogite	eclogite

Abbreviations are after Kretz (1983).

Table 2

Analytical data for selected Raspas Metamorphic Complex lithologies

La Chilca Unit: mafic igneous rocks							
	Eclogite metabasalt	Amphibole	Clinopyroxene	Garnet	Eclogite metabasalt	Eclogite metabasalt	Gt amphibolite metagabbro
Sample number	97CE1	97CE1	97CE1	97CE1	98RR4	98RR6	97CE4A
SiO <sub>2</sub>	49.6 <sup>a</sup>	nd	nd	nd	47.05	50.41	47.57 <sup>a</sup>
TiO <sub>2</sub>	1.48	nd	nd	nd	1.2	2.45	0.46
Al <sub>2</sub> O <sub>3</sub>	15.08	nd	nd	nd	15.2	16.95	17.11
Fe <sub>2</sub> O <sub>3</sub>	12.44	nd	nd	nd	13.55	9.4	8.12
MnO	0.21	nd	nd	nd	0.25	0.18	0.17
MgO	7.58	nd	nd	nd	9.08	5.97	10.36
CaO	10.68	nd	nd	nd	9.45	7.03	12.29
Na <sub>2</sub> O	2.32	nd	nd	nd	1.95	4.07	2.28
K <sub>2</sub> O	0.08	nd	nd	nd	0.95	0.87	0.08
P <sub>2</sub> O <sub>5</sub>	0.15	nd	nd	nd	0.11	0.51	0.02
LOI	0.31	nd	nd	nd	0.34	1.38	nd
Total	100.01	nd	nd	nd	99.13	99.33	98.47
Sc	75	nd	nd	nd	nd	nd	50
V	602.2	nd	nd	nd	nd	nd	180.7
Cr	172.61	nd	nd	nd	nd	nd	542.8
Ni	58.67	nd	nd	nd	nd	nd	31.8
Rb	0.55	0.14	1.3	nd	3.32	18.13	0.8
Sr	88	28	9.21	nd	74.37	55.99	132
Ba	22.00 <sup>b</sup>	9.82 <sup>b</sup>	22 <sup>b</sup>	nd	131.53	482.39	32.67 <sup>b</sup>
U	0.17	0.01	0.07	nd	0.32	0.34	0.17
Th	0.48	0.035	0.2	nd	0.37	0.35	bdl
Pb	0.55	bdl	0.012	nd	0.67	3.28	9.83
Hf	2.31	0.26	0.34	nd	2.34	2.04	0.39
Zr	90.55	3.07	4.25	nd	84.04	74.32	10.73
Ta	0.48	0.067	0.065	nd	0.33	0.31	0.02
Nb	8.5	1.1	1.11	nd	5.27	5.09	0.29
Y	35.83	6.5	5.7	nd	32.52	29.95	13.44
La	6.39	0.31	1.99	nd	4.69	4.612	0.91
Ce	15.53	0.79	4.89	0.001 <sup>a</sup>	12.18	11.08	2.33
Pr	2.29	0.12	0.75	nd	1.93	1.802	0.41
Nd	10.79	0.60	3.60	0.01	9.78	9.18	2.4
Sm	3.43	0.22	1.13	0.047	3.24	3.119	1.03
Eu	1.12	0.08	0.41	0.20	1.07	1.105	0.6
Gd	3.91	0.37	1.53	0.80	4.29	4.64	1.43
Tb	0.8	0.09	0.26	nd	0.80	0.78	0.3
Dy	5.44	0.81	1.50	9.37	5.44	5.10	2.02
Ho	1.21	0.22	0.27	nd	1.21	1.12	0.46
Er	3.37	0.67	0.53	28.71	3.31	3.01	1.28
Tm	0.53	0.09	0.05	nd	nd	nd	0.19
Yb	3.54	0.55	0.24	40.6	3.40	3.09	1.21
Lu	0.53	0.07	0.03	45.07	0.53	0.49	0.18
<sup>87</sup> Sr/ <sup>86</sup> Sr	0.706533 ± 15	0.703938 ± 14	0.704180 ± 12	nd	nd	nd	0.705226 ± 12
( <sup>87</sup> Sr/ <sup>86</sup> Sr) <sub>i</sub> <sup>c</sup>	0.70649	0.70391	0.70331				0.70519
<sup>143</sup> Nd/ <sup>144</sup> Nd	0.513074 ± 05	0.513017 ± 07	0.513039 ± 11	nd	0.513143 ± 05	0.512881 ± 05	0.513104 ± 05
( <sup>143</sup> Nd/ <sup>144</sup> Nd) <sub>i</sub> <sup>c</sup>	0.51289	0.51280	0.51285		0.51295	0.51268	0.51285
εNd <sub>i</sub>	+ 8.59	+ 6.92	+ 7.96		+ 9.79	+ 4.58	+ 7.89
( <sup>208</sup> Pb/ <sup>204</sup> Pb) <sub>i</sub> <sup>c</sup>	38.249	nd	37.934	nd	38.020	38.803	38.273
( <sup>207</sup> Pb/ <sup>204</sup> Pb) <sub>i</sub> <sup>c</sup>	15.561		15.505		15.513	15.663	15.598
( <sup>206</sup> Pb/ <sup>204</sup> Pb) <sub>i</sub> <sup>c</sup>	18.691		18.229		18.190	18.567	18.358

Table 2 (continued)

La Chilca Unit: sedimentary rocks							
	Metapelite	Metapelite whole Rock	Phengite	Grt with inclusions	Metapelite whole Rock	Metapelite whole rock	Metapelite whole rock
Sample number	97CE2	97CE3	97CE3	97CE3	97CE4	97CE5	97CE6
SiO <sub>2</sub>	72.14 <sup>a</sup>	74.3	nd	nd	70.05	76.03	76.86 <sup>a</sup>
TiO <sub>2</sub>	0.46	0.52	nd	nd	0.73	0.82	0.88
Al <sub>2</sub> O <sub>3</sub>	12.9	11.87	nd	nd	13.86	13.05	12.45
Fe <sub>2</sub> O <sub>3</sub>	5.26	5.71	nd	nd	6.56	4.15	4.68
MnO	0.14	0.07	nd	nd	0.08	bdl	0.03
MgO	1.26	1.28	nd	nd	1.46	0.45	0.54
CaO	0.51	0.69	nd	nd	0.81	0.18	0.28
Na <sub>2</sub> O	0.84	0.63	nd	nd	0.88	0.68	0.58
K <sub>2</sub> O	2.22	1.88	nd	nd	1.94	1.31	1.27
P <sub>2</sub> O <sub>5</sub>	0.18	0.09	nd	nd	0.13	0.08	0.1
LOI	nd	2.84	nd	nd	3.4	3.11	nd
Total	96.17	99.88	nd	nd	99.9	99.86	97.68
Sc	24	nd	nd	nd	nd	nd	18
V	278	nd	nd	nd	120	71	71
Cr	122.8	nd	nd	nd	94	62	61.3
Ni	8.6	nd	nd	nd	25	12	7.8
Rb	82.8	78.78	309.3	4.58	40.14	18.74	49.9
Sr	97.7	71.7	178.77	3.06	70.08	15.57	74.9
Ba	1547	607.98	2469.96	28.69	362.93	56.35	334.3
U	1.802	1.16	0.6	0.42	1.47	1.10	1.35
Th	9.804	5.79	3.24	1.17	6.52	1.96	4.87
Pb	16.19	14.01	43.91	1.12	14.32	12.25	12.73
Hf	4.93	0.25	0.07	1.36	1.31	3.53	8.67
Zr	159.8	9.55	2.09	53.01	51.3	137.43	318.3
Ta	0.752	0.53	0.08	0.25	0.9	1.17	0.95
Nb	10.18	8.16	1.83	3.26	14.01	17.43	14.02
Y	34.2	27.41	2.18	167.26	31.66	9.58	17.3
La	21.08	20.68	15.05	3.53	27.13	9.07	16.89
Ce	38.11	42.26	30.88	6.69	61.38	28.8	29.07
Pr	nd	5.3	3.85	0.9	7.2	2.65	nd
Nd	20.95	19.97	14.23	3.55	27.81	9.71	13.57
Sm	4.32	4.05	2.73	1.88	5.61	1.95	2.73
Eu	0.96	0.96	0.73	1	1.26	0.42	0.65
Gd	4.16	4.08	1.96	8.31	5.22	1.66	3.06
Tb	nd	0.65	0.18	2.68	0.8	0.27	nd
Dy	5.4	4.08	0.62	22.23	4.81	1.66	3.45
Ho	nd	0.88	0.08	5.53	1.03	0.34	nd
Er	3.47	2.63	0.17	17.66	3.03	1.06	1.93
Tm	nd	nd	nd	nd	nd	nd	nd
Yb	3.54	2.62	0.13	19.58	3.11	1.24	2.08
Lu	0.55	0.42	0.02	3.14	0.49	0.2	0.32
<sup>87</sup> Sr/ <sup>86</sup> Sr	nd	0.722593 ± 16	nd	nd	nd	0.721221 ± 16	nd
( <sup>87</sup> Sr/ <sup>86</sup> Sr) <sub>i</sub> <sup>c</sup>		0.71581				0.71379	
<sup>143</sup> Nd/ <sup>144</sup> Nd	nd	0.512240 ± 11	nd	nd	0.512126 ± 05	0.512079 ± 08	nd
( <sup>143</sup> Nd/ <sup>144</sup> Nd) <sub>i</sub> <sup>c</sup>		0.51212			0.51201	0.51196	
εNd <sub>i</sub>		- 6.35			- 8.56	- 9.47	
( <sup>208</sup> Pb/ <sup>204</sup> Pb) <sub>i</sub> <sup>c</sup>	nd	38.774	nd	39.653	38.780	38.890	38.910
( <sup>207</sup> Pb/ <sup>204</sup> Pb) <sub>i</sub> <sup>c</sup>		15.700		15.688	15.700	15.710	15.708
( <sup>206</sup> Pb/ <sup>204</sup> Pb) <sub>i</sub> <sup>c</sup>		18.925		19.657	18.907	18.972	18.957

(continued on next page)



Table 2 (continued)

	El Toro Unit: ultramafic rocks			Rio Panupili unit: mafic rocks			
	Serpentine	Duplicate	Harzburgite	Amphibolite metabasalt	Amphibolite metagabbro	Amphibolite metabasalt	Amphibolite metabasalt
	97CE14	97CE14	97CE15	97CE18	97CE13	98TH13	97CE12
SiO <sub>2</sub>	40.08 <sup>d</sup>		40.97	50.59 <sup>d</sup>	49.92 <sup>d</sup>	48.76	48.95
TiO <sub>2</sub>	0.09		0.08	1.42	0.77	1.16	1.41
Al <sub>2</sub> O <sub>3</sub>	2.81		2.98	13.96	17.42	14.64	14.91
Fe <sub>2</sub> O <sub>3</sub>	8.25		8.27	10.31	7.35	10.25	10.62
MnO	0.1		0.11	0.17	0.11	0.16	0.19
MgO	37.04		36.67	7.51	7.65	8.19	8.02
CaO	2.5		2.38	10.5	10.07	11.9	10.22
Na <sub>2</sub> O	0.05		0.5	3.01	3.28	3.01	2.89
K <sub>2</sub> O	0.01		bdl	0.1	0.18	0.1	0.13
P <sub>2</sub> O <sub>5</sub>	0.01		0.07	0.14	0.08	0.1	0.13
LOI	8.65		8.22	1.6	3.01	1.23	3.01
Total	99.78		99.8	99.41	99.49	99.48	99.49
Sc	11.32	nd	nd	40.26	27.07	nd	27.07
V	81.31	nd	nd	355.65	210.52	nd	210.51
Cr	2614.01	nd	nd	199.34	396.10	nd	48.95
Ni	7112.94	nd	nd	nd	nd	nd	nd
Rb	0.35	0.38	0.69	1.13	2.50	1.89	1.07
Sr	12.46	12.8	10.58	124.90	200.70	116.94	119.99
Ba	nd	6.16	0.01	10.83	8.31	29.82	10.36
U	0.013 <sup>b</sup>	bdl	0.01	0.04 <sup>b</sup>	nd <sup>b</sup>	0.12	0.048
Th	0.026	0.02	0.03	0.12	0.011	0.08	0.11
Pb	2.26	nd	0.53	2.72	3.19	1.14	66.63
Hf	0.074	0.11	0.09	32.05	17.28	1.82	0.82
Zr	2.17	2.97	1.54	1.03	0.69	52.89	22.31
Ta	0.005	0.01	bdl	0.17	0.023	0.16	0.1
Nb	0.43	0.66	1.65	2.50	0.38	2.31	1.01
Y	2.27	2.39	2.68	31.18	14.53	42.18	3.03
La	0.53	0.51	0.25	3.74	1.19	3.58	4.65
Ce	0.89	0.87	0.42	12.30	3.87	11.19	12.89
Pr	0.10	0.1	0.05	2.05	0.68	2.06	2.09
Nd	0.40	0.43	0.28	10.38	3.97	11.26	10.08
Sm	0.14	0.15	0.15	3.45	1.37	4.01	3.27
Eu	0.11	0.11	0.13	1.37	0.56	1.36	1.27
Gd	0.23	0.26	0.26	4.33	1.84	5.11	4.16
Tb	0.05	0.05	0.06	0.79	0.34	0.99	0.76
Dy	0.33	0.35	0.4	5.15	2.31	6.91	5.08
Ho	0.077	0.08	0.1	1.12	0.50	1.49	1.09
Er	0.24	0.26	0.29	3.17	1.47	4.04	3.15
Tm	nd	nd	nd	2.28	2.21	nd	2.93
Yb	0.25	0.25	0.31	3.00	1.40	4.10	3.03
Lu	0.04	0.04	0.05	0.44	0.21	0.63	0.44
<sup>87</sup> Sr/ <sup>86</sup> Sr	0.704242±13	nd	0.704183±12	0.704019±07	0.703137±06	nd	0.70335±6
( <sup>87</sup> Sr/ <sup>86</sup> Sr) <sub>i</sub> <sup>c</sup>	0.70407		0.70378	0.70396	0.70306		0.703280
<sup>143</sup> Nd/ <sup>144</sup> Nd	nd	nd	0.513175±19	0.513160±07	0.513170±13	0.513198±07	0.513191±6
( <sup>143</sup> Nd/ <sup>144</sup> Nd) <sub>i</sub> <sup>c</sup>			0.51286	0.51296	0.51296	0.51299	0.512998
εNd <sub>i</sub>			+8.04	+10.11	+10.14	+10.57	+10.8
( <sup>208</sup> Pb/ <sup>204</sup> Pb) <sub>i</sub> <sup>c</sup>	37.804	nd	38.457	nd	37.705	37.689	nd
( <sup>207</sup> Pb/ <sup>204</sup> Pb) <sub>i</sub> <sup>c</sup>	15.442		15.524		15.477	15.480	
( <sup>206</sup> Pb/ <sup>204</sup> Pb) <sub>i</sub> <sup>c</sup>	18.126		18.674		18.058	17.941	

fault system belong to the El Toro unit. The studied samples (97Ce14, 97Ce15) were collected close to the village of Limón Playa (Fig. 2, UTM-WGS84: 17/618250E-9604200N). Most olivine porphyroblasts are transformed into serpentine aggregates. Preserved crystals correspond to Mg-rich olivine (Fo90). Fibrous aggregates of colourless amphibole underlie a rather well developed schistosity. Recent observations suggest that the harzburgites of the El Toro unit underwent HP metamorphic conditions (Gabriele and Piccardo, in preparation).

The epidote bearing amphibolites were sampled in the “Quebrada de Damas” (97Ce12, UTM-WGS84: 17/625500E-9597500N), 0.8 km W of the village of Zaracay (97Ce18), and in a quarry located 1.8 km W of Zaracay (98TH13, UTM-WGS84: 17/624748E-9596892N). They show an association of actinolite, chlorite and epidote typical of the greenschist facies metamorphism. All samples have a well defined schistosity. An amphibolite (metagabbro) (97Ce13) in which green hornblende porphyroblasts underline a poorly developed cleavage was also collected in the Quebrada de Damas North of the Zaracay village (Fig. 2).

### 3.2. The metapelites

The metapelites (97Ce2 to 97Ce6) were sampled in the mentioned Río Raspas, where they are closely associated with the eclogites (Fig. 2). The metapelites are medium-to coarse-grained graphite bearing garnet-micaschists, where the eclogitic paragenesis consists of quartz, white mica, garnet, chloritoid, kyanite and rutile. The white mica defines the main schistosity, within which garnet poikiloblasts developed. This latter includes quartz, kyanite, chloritoid and rutile inclusions. Peak metamorphic conditions for the metapelites reached approximately 600 °C and 20 kbar (Gabriele et al., 1999).

## 4. Analytical procedures

Trace element abundances have been determined by solution- and selective laser ablation (LA)-ICP-MS for amphibole, omphacite, phengite and garnet separates and garnet in thick-section from a mafic eclogite and pelitic schists. LA-ICP-MS analyses were performed at School of Earth Sciences at the Australian National University. Solution trace element analyses were performed by inductively coupled plasma mass spectrometry (ICP-MS) at the Université Joseph Fourier (Grenoble) after acid digestion. Trace elements are spiked with pure Tm using procedures described by Barrat et al. (1996). Standards JB2, WSE, BIR-1, JR1, and UBN were analyzed together with unknown samples. Major element analyses were performed at the Centre de Recherche Pétrographiques et Géochimiques (CRPG, Nancy).

Isotopic data (Sr, Nd and Pb) have been obtained for almost all the lithologies. The  $^{143}\text{Nd}/^{144}\text{Nd}$  and  $^{87}\text{Sr}/^{86}\text{Sr}$  isotopic compositions were measured on a Finnigan MAT261 multicollector mass spectrometer at the Laboratoire de Géochimie de l'Université Paul Sabatier, using the analytical procedures of Lapiere et al. (1997). The chemical separation of lead was done at the Laboratoire de Géochimie de l'Université de Montpellier II following a procedure modified from Manhès et al. (1978). Total Pb blanks are less than 65 pg for a 100 mg sample. The Pb/Pb isotopic ratios were measured on the MC-ICP-MS P54 at the Ecole Nationale Supérieure de Lyon.

The complete isotopic data set has been corrected for in situ decay assuming an age of 150 Ma, based on the median age of the Amotape–Chaucha Terrane (ACT) lithologies (Litherland et al., 1994).

Analytical data for representative lithologies of the Raspas Metamorphic Complex are presented in Table 2.

---

Notes to Table 2:

$\epsilon\text{Nd}_i$  calculated with actual  $(^{143}\text{Nd}/^{144}\text{Nd})_{\text{CHUR}} = 0.512638$  and  $(^{147}\text{Sm}/^{144}\text{Nd})_{\text{CHUR}} = 0.1967$  (Wasserburg et al., 1981).

Pb isotopic ratios measured with external precision of ca. 100–150 ppm for the  $^{206}\text{Pb}/^{204}\text{Pb}$ ,  $^{207}\text{Pb}/^{204}\text{Pb}$  ratios.

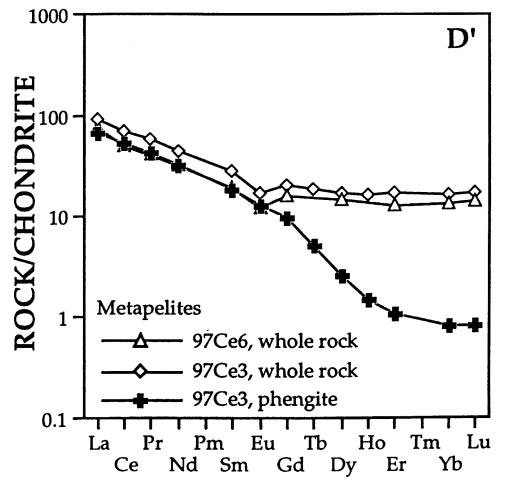
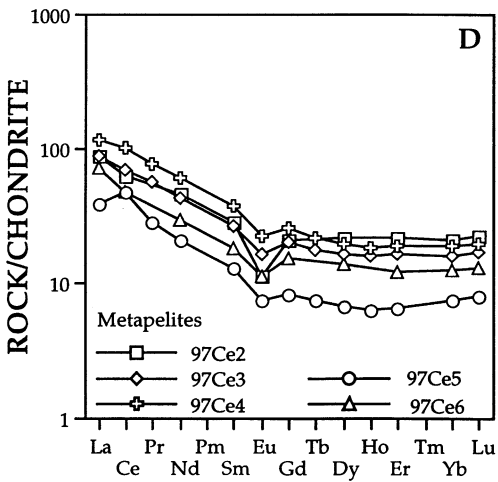
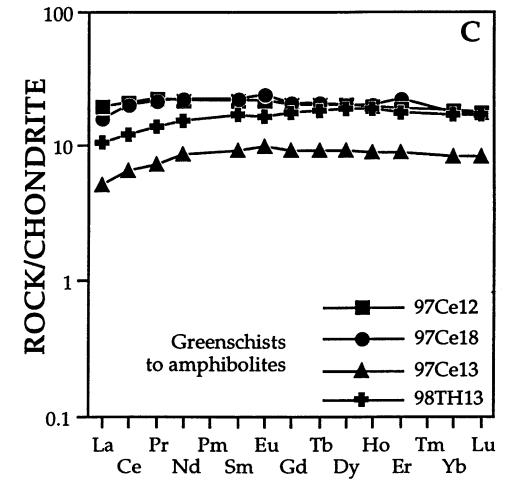
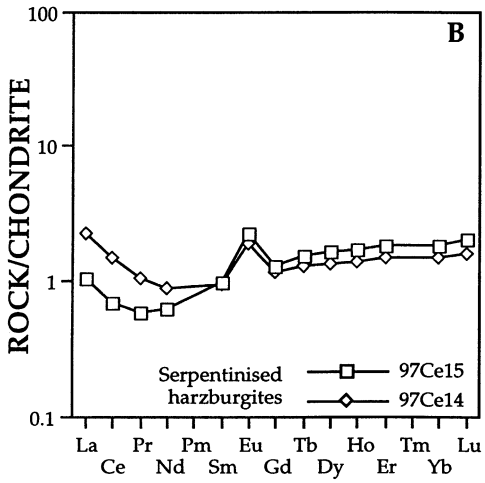
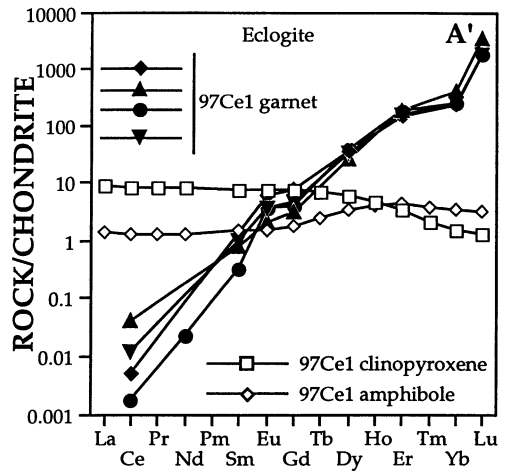
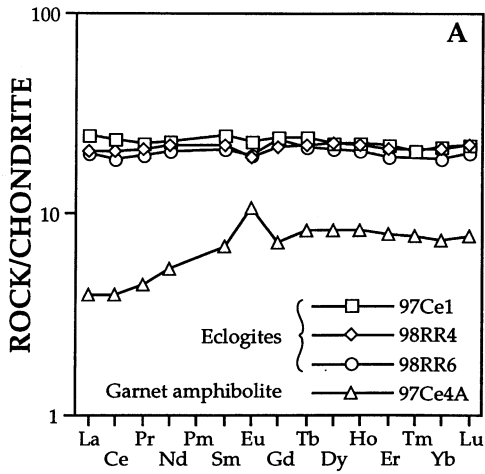
Abbreviations: nd, not determined; bdl, below detection limit.

<sup>a</sup> Major and trace elements analyses performed at the Department of Geology and Research School of Earth Sciences, ANU.

<sup>b</sup> Trace element analyses (ppm) performed at the Laboratoire des Chaînes Alpines, Univ. Joseph Fourier (Grenoble, France).

<sup>c</sup> All isotopic data ( $2\sigma$  error) are corrected for in situ decay assuming an age of 150 Ma (Litherland et al., 1994).

<sup>d</sup> Major (%) and Sc, V, Cr, Ni (ppm) analyses performed at the Laboratoire Pétrologie, Univ. Claude Bernard (Lyon, France).



## 5. Geochemistry of rocks of the Raspas Metamorphic Complex

### 5.1. Eclogites (97Ce1, 98RR4, 98RR6) and garnet amphibolite (97Ce4A)

Eclogites are very fresh rocks (LOI < 1.4%) with homogeneous major and trace element compositions (Table 2). The MgO contents (from 6% to 9.1%) are similar to those of fractionated basalts while the TiO<sub>2</sub> and Fe<sub>2</sub>O<sub>3</sub> contents as well as La/Nb (0.75–0.91) and La/Th (12.68–13.42) ratios display enriched MORB signature.

Chondrite-normalised (CN; Sun and McDonough, 1989) patterns for eclogites and mineral separates are presented in Fig. 3A and A'. The REE abundances of these rocks are 20 times the chondritic values and their REE patterns are flat [ $0.99 < (La/Yb)_{CN} < 1.29$ ;  $0.88 < (Ce/Sm)_{CN} < 1.13$ ], suggesting an Oceanic Plateau Basalt (OPB) affinity (Kerr et al., 1997). These eclogites have Eu negative anomalies [ $0.64 < Eu/Eu^* < 0.88$ ]. 97Ce1 clinopyroxene and barroisite separates have lower REE abundances than the host rock. Clinopyroxene differs from the amphibole by a strong LREE enrichment [ $(La/Yb)_{CN} = 5.92$ ]. Conversely, the amphibole is enriched in HREE, compared to the pyroxene [ $(La/Yb)_{CN} = 0.41$ ].

Primitive mantle-normalised multi-elements plots of the Raspas eclogites are flat with the exception of large ion lithophile elements (LILE). Pb and Th show positive or negative anomalies depending on the rock lithologies (Fig. 4A). All eclogites exhibit negative Sr anomalies. 97Ce1, which does not contain phengite minerals, is relatively depleted in Rb, Ba and Pb contrasting with the two other eclogites (98RR4 and 98RR6) that are enriched in Rb and Ba. In addition, 98RR6 differs from the other eclogites by higher Pb and TiO<sub>2</sub> contents. The absence or presence of phengites in the eclogites often determines the K, Ba and Rb abundances of the rock (Becker et al., 2000).

It is slightly different for Pb where the content of this element in the eclogite depends on more than

one mineral. Pb may substitute for K in phengite, it substitutes for Ca in epidote-group minerals (epidote, zoisite, clinozoisite) and may also replace Na in paragonite. Thus, the multi-element distribution in the eclogites can be substantially influenced by the nature of the protolith, by the mineral assemblage, as well as by the impact of element partitioning of phases with high LILE or HFSE abundances (such as rutile). Similarly, the Nb/U and Ce/Pb of the eclogites are highly variable. The Nb/U (51.1) and Ce/Pb (28.4) of the phengite-free eclogite (97Ce1) approach those of unaltered MORB or OIB (Hofmann et al., 1986). In contrast, these ratios are significantly lower in the phengite-bearing eclogites [ $15.0 < Nb/U < 16.5$ ;  $3.4 < Ce/Pb < 18.2$ ]. The U and Nb contents of eclogites may be partly controlled by the occurrence and abundance of specific minerals such as garnet and omphacite (for U<sup>4+</sup>) and rutile (for U<sup>6+</sup> and Nb) (Brenan et al., 1994).

Bulk rock major element composition of the garnet-amphibolite (97Ce4A) is similar to that of a cumulate gabbro (Table 2). The REE pattern of this rock has a marked LREE depletion [ $(La/Yb)_{CN} = 0.54$ ;  $(Ce/Sm)_{CN} = 0.56$ ] and an Eu positive anomaly [ $Eu/Eu^* = 1.5$ ] suggesting that the protolith was formed by the accumulation of cpx and plagioclase (Fig. 3A). This is confirmed by the high Al<sub>2</sub>O<sub>3</sub> (17.1%) and Cr (543 ppm) contents of this rock (Table 2). Primitive mantle-normalised multi-elements plot of this garnet amphibolite (Fig. 4A) supports this interpretation with a marked depletion in the most incompatible elements (Nb, Ta, Zr, Hf). This metamorphic rock is also depleted in Rb but enriched in Pb and Sr. Positive anomalies for these two latter elements are likely related to plagioclase accumulation, suggesting that high-pressure metamorphism had little effect on the primary chemical composition of the rock.

The Sr isotopic compositions of the garnet-amphibolite (97Ce4A) and eclogite (97Ce1) and their corresponding cpx and amphibole have been measured (Table 2). 97Ce1 whole-rock and cpx have the highest and lowest (<sup>87</sup>Sr/<sup>86</sup>Sr)<sub>i</sub> ratios (0.70649 and 0.70331,

Fig. 3. Chondrite-normalized (CN) rare element patterns of the minerals and host rocks from the Raspas metamorphic rocks. (A) Eclogites and garnet-amphibolite (97Ce4A); (A') mineral separates from the 97Ce1 eclogite; (B) serpentinised harzburgites; (C) greenschists and amphibolites; (D) high-pressure metasedimentary rocks; (D') mineral separates from the metapelites (97Ce3 and 97Ce6).

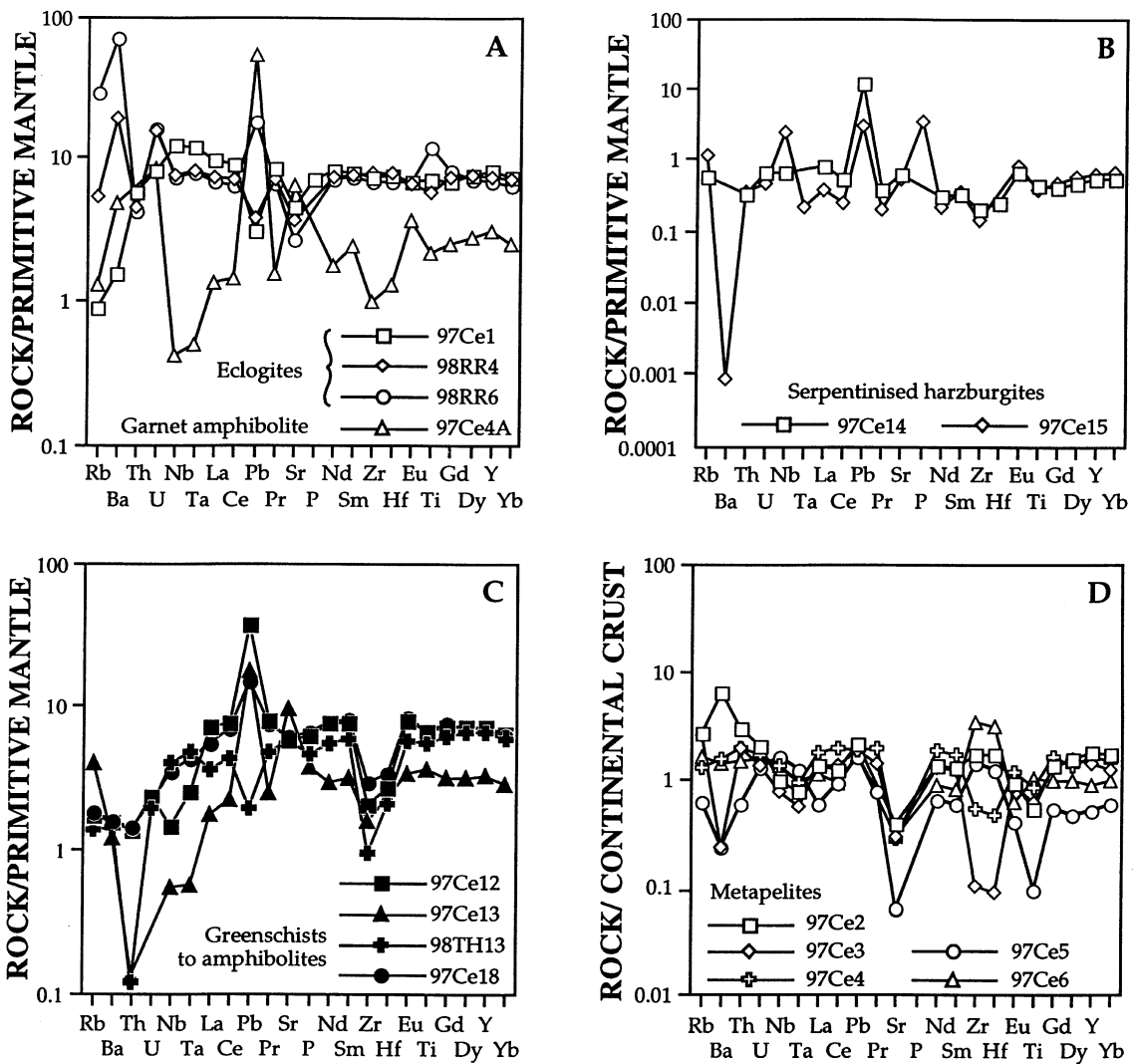


Fig. 4. Multi-trace-element patterns for the whole rocks from the Raspas metamorphic rocks. (A) Primitive Mantle (PM)-normalised plots for the eclogites and garnet-amphibolite (97Ce4A); (B) (PM) plots for the serpentinitised harzburgites; (C) (PM) plots for the amphibolites; (D) Bulk Continental Crust (BCC)-normalised plots for the metapelites.

respectively), while that of the amphibole is slightly higher (0.70391) than the cpx value.  $(^{87}\text{Sr}/^{86}\text{Sr})_i$  of the garnet-amphibolite is significantly lower than that of the 97Ce1 eclogite (0.70519).

Eclogites, mineral separates and garnet-amphibolite  $\epsilon\text{Nd}_i$  range from +4.58 to +9.79 (Table 2). Reported in the  $\epsilon\text{Nd}_i$  versus  $(^{87}\text{Sr}/^{86}\text{Sr})_i$  (Fig. 5A), they fall in the N-MORB and OIB fields. One out of four of these high-pressure metamorphic rocks

(98RR6) exhibits a significantly lower  $\epsilon\text{Nd}_i$  (+4.58). In these rocks, no clear correlation is observed between  $\epsilon\text{Nd}_i$  and (La/Yb) ratio (Fig. 5B). In Fig. 5A, the lateral shift observed for the  $^{87}\text{Sr}/^{86}\text{Sr}$  ratios of 97Ce1 and 97Ce4A whole rocks, without any decrease of the  $\epsilon\text{Nd}_i$ , could be attributed to a hydrothermal alteration or could result from altered oceanic crust assimilation. Initial lead isotopic compositions of these samples are scattered (Table 2) and display

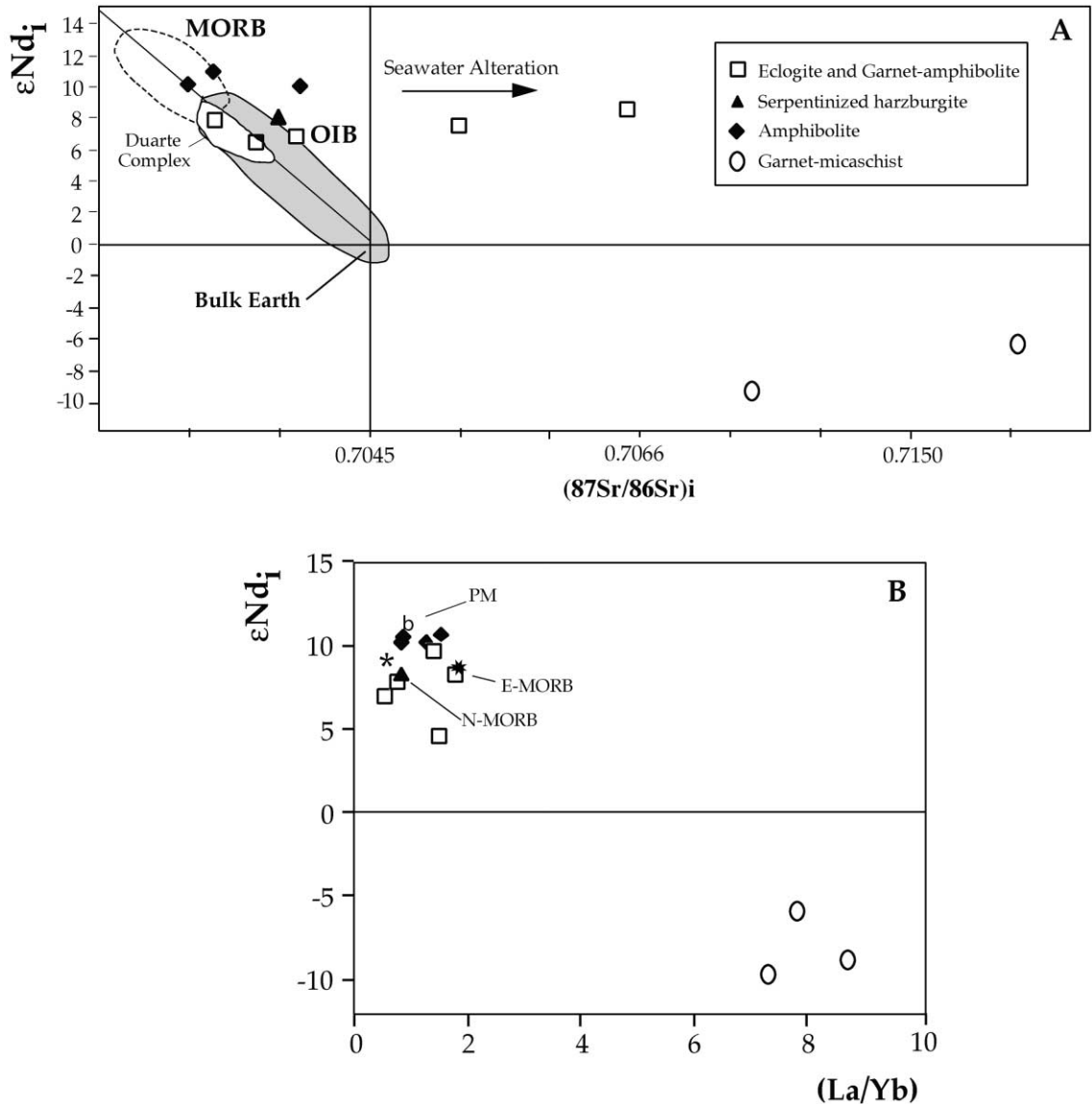


Fig. 5. (A)  $\epsilon Nd_i$  versus  $(^{87}Sr/^{86}Sr)_i$  diagram for rocks of the Raspas Metamorphic Complex (this study). The field of the Duarte Complex basalts and cumulates has been reported for comparison (Lapierre et al., 2000); (B)  $\epsilon Nd_i$  versus  $(La/Yb)$  diagram.  $La/Yb$  ratios for E-MORB, N-MORB and Primitive Mantle (PM) are taken from Sun and McDonough (1989).

typical MORB and/or OIB signature. Two samples (98RR6 and 97Ce4A), however, exhibit significantly higher Pb/Pb values (Fig. 6). This feature could be due to contribution of a radiogenic component, which may be assimilated to continental crust or pelagic sediments or to a strong seawater hydrothermal alteration. The lowest lead isotopic composition has been

obtained on cpx from the 97Ce1 eclogite, which plots in the N-MORB domain.

### 5.2. Serpentinised harzburgites (97Ce14, 97Ce15)

The bulk rock compositions of the serpentinised ultramafic rocks are typical to those of harzburgites

with very low  $\text{Al}_2\text{O}_3$ , CaO and  $\text{TiO}_2$  contents and very high MgO amounts (Table 2). The high LOI (>8%) testifies to the alteration degree of these rocks and to the abundance of serpentinite after olivine and orthopyroxene pseudomorphs. High Cr content (2641 ppm for 97Ce14) is due to the occurrence of preserved Cr-rich chromite spinels (picotite). Chondrite-normalised REE patterns of these ultramafic rocks are characterized by La and Ce enrichments [ $1.76 < (\text{La}/\text{Nd})\text{CN} < 2.58$ ] and positive Eu anomalies [ $1.78 < \text{Eu}/\text{Eu}^* < 2.04$ ] (Fig. 3B). The medium to heavy REE are within the range expected for residual ultramafic lithologies remaining after basalt extraction. The LREE and Eu enrichments may reflect a more complex origin but can also be related to late hydrothermal alteration. Ultramafic rocks (primitive mantle normalized) multi-element plots show trace element contents close to the primitive mantle abundances with the exception of Pb, which is slightly enriched in both samples (Fig. 4B). 97Ce15 also exhibits a significant negative Ba anomaly and more limited positive Nb and P anomalies relative to 97Ce14 and the primitive mantle. Both ultramafic rocks possess ( $^{87}\text{Sr}/^{86}\text{Sr}$ )<sub>i</sub> ratios which fall in the range of the Raspas mafic amphibolites (Table 2, Fig. 5A).  $\epsilon\text{Nd}_i$  ratio of 97Ce15 (+8.04) is similar to those of most of the Raspas eclogites but is significantly lower than those of abyssal harzburgites (Snow et al., 1994). In Fig. 5A,B, 97Ce15 (black triangle) plots close to the less hydrothermally altered eclogites. Reported in Fig. 6, the initial lead isotopic ratios of the serpentinitised harzburgites plot on or close to the NHRL (Hart, 1984) and fall in the MORB field.

### 5.3. Greenschists to amphibolite metamorphic rocks (97Ce12, 97Ce13, 97Ce18, 98TH13)

Amphibolites bulk rock major and trace element compositions are similar to those of N-MORB. They are LREE depleted [ $0.61 < (\text{La}/\text{Yb})\text{CN} < 0.90$ ;  $0.70 < (\text{Ce}/\text{Sm})\text{CN} < 0.89$ ] and relatively flat for medium to heavy REE [ $0.70 < (\text{Sm}/\text{Yb})\text{CN} < 1.85$ ] (Fig. 3C). 97Ce13 differs from the metabasalts by lower REE and  $\text{TiO}_2$  abundances, higher  $\text{Al}_2\text{O}_3$  content and a very slight positive Eu anomaly ( $\text{Eu}/\text{Eu}^* = 1.09$ ), suggesting that the protolith was a plagioclase cumulate gabbro. Primitive mantle normal-

ised multi-element plots of these amphibolites confirm their N-MORB affinities (Fig. 4C) with large depletions in LILE, Th, Zr and Hf. Positive Pb, Sr and Eu anomalies in samples 97Ce12, 97Ce13 and 97Ce18 likely reflect plagioclase accumulation, suggesting that these elements were not intensely mobilised during metamorphism. ( $^{87}\text{Sr}/^{86}\text{Sr}$ )<sub>i</sub> ratios of these amphibolites do not significantly differ from those of the serpentinitised harzburgites of the El Toro unit (Table 2). The metagabbro and metabasalts yield very similar  $\epsilon\text{Nd}_i$  ratios ( $+10.11 < \epsilon\text{Nd}_i < +10.81$ ), in the typical range of MORB (Fig. 5A). They are significantly more radiogenic than those of the eclogites and serpentinitised harzburgite. In the  $\epsilon\text{Nd}_i$ -(La/Yb)CN diagram (Fig. 5B), these amphibolites exhibit the highest  $\epsilon\text{Nd}_i$  and the most LREE-depleted patterns of all analyzed rocks from the Raspas Metamorphic Complex. The ( $^{206}\text{Pb}/^{204}\text{Pb}$ )<sub>i</sub>, ( $^{207}\text{Pb}/^{204}\text{Pb}$ )<sub>i</sub> and ( $^{208}\text{Pb}/^{204}\text{Pb}$ )<sub>i</sub> ratios of the 98TH13 and 97Ce13 amphibolites are very similar to the 97Ce14 serpentinite and are located in the more depleted part of the MORB domain (Fig. 6).

### 5.4. Garnet-micaschists (97Ce2, 97Ce3, 97Ce4, 97Ce5, 97Ce6)

Metapelites have very homogeneous major element compositions, close to that of continental crust (Taylor and McLennan, 1985). Differences in  $\text{TiO}_2$  and MgO contents are likely to be linked to the abundance of oxides. The REECN patterns of these metapelitic rocks are similar to that of the Bulk Continental Crust (BCC), (Taylor and McLennan, 1985; Fig. 3D) with a characteristic LREE-enrichment [ $4.27 < (\text{La}/\text{Yb})\text{CN} < 6.26$ ] and a marked negative Eu anomaly [ $0.46 < \text{Eu}/\text{Eu}^* < 0.91$ ]. 97Ce5 differs from the other rocks by a positive Ce anomaly [ $\text{Ce}/\text{Ce}^* = 1.44$ ], which could be linked to seawater alteration. 97Ce3 phengite differs from its related host rock by a significantly higher (La/Yb)CN ratio (83.04) (Fig. 3D'). The difference between the whole-rock and phengite pattern is attributed to the presence of garnet in the bulk rock, which balanced the strong HREE depletion of the phengite. Most of the trace element abundances of these metapelites are similar to those of BCC, as emphasized by the essentially nonfractionated Bulk Continental Crust normalized-patterns reported in Fig. 4D. However,

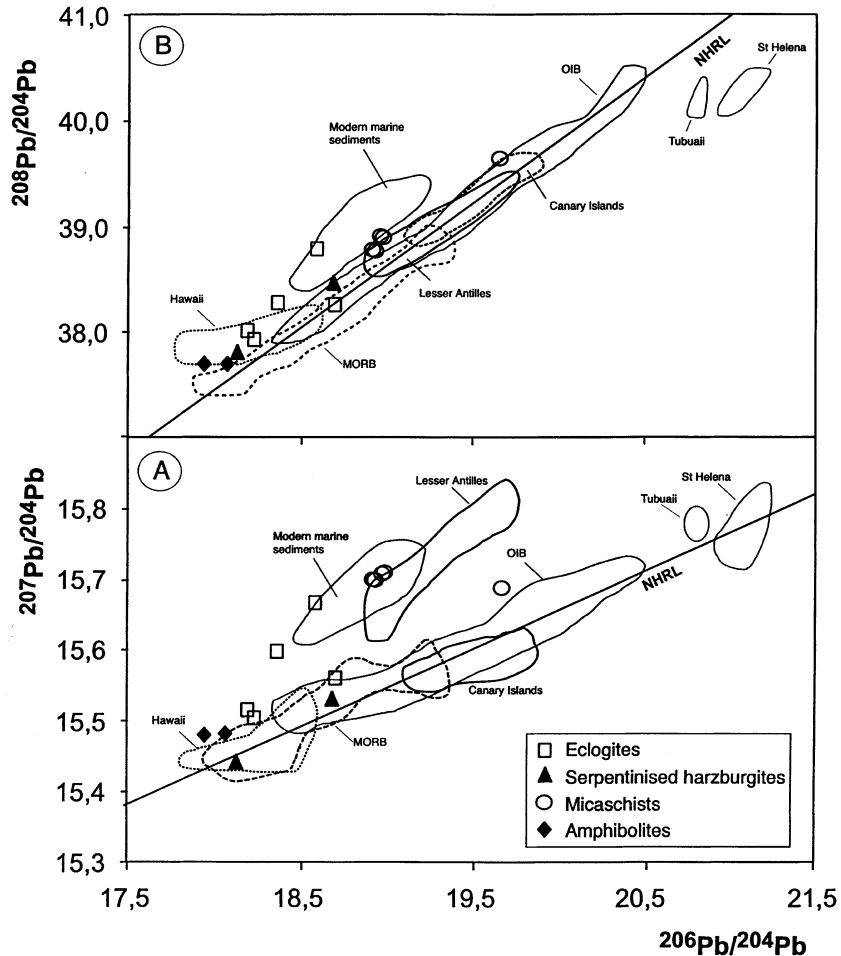


Fig. 6. Correlation plots of (A)  $^{206}\text{Pb}/^{204}\text{Pb}$  versus  $^{207}\text{Pb}/^{204}\text{Pb}$  and (B)  $^{206}\text{Pb}/^{204}\text{Pb}$  versus  $^{208}\text{Pb}/^{204}\text{Pb}$  for rocks of the Raspas Metamorphic Complex. Data sources for OIBs (Hart et al., 1986; Stille et al., 1986; White et al., 1993); St-Helena (Newson et al., 1986); Tubuaii (Vidal et al., 1984), Lesser Antilles (Davidson, 1987), Canary Islands (Hoernle and Tilton, 1991); MORB (White et al., 1987; Mahoney et al., 1989; Staudigel et al., 1991), Modern marine sediments (Ben Othman et al., 1989); NHRL, Northern Hemisphere Reference Line (Hart, 1984).

abundances of Ba, Th, Zr and Hf differ from one rock to another (Fig. 4D). Relative to BCC,  $^{97}\text{Ce}2$  is enriched in Ba and Th while  $^{97}\text{Ce}5$  and  $^{97}\text{Ce}3$  are strongly depleted.  $^{97}\text{Ce}6$  and  $^{97}\text{Ce}3$  are enriched and depleted in Zr and Hf, respectively. Losses in Sr affect all the metapelites. The  $(^{87}\text{Sr}/^{86}\text{Sr})_i$ ,  $\epsilon\text{Nd}_i$  and  $(^{206}, ^{207}, ^{208}\text{Pb}/^{204}\text{Pb})_i$  ratios of the metapelites are homogeneous and typical of the continental crust (Figs. 5A and 6). The negative  $\epsilon\text{Nd}_i$  values ( $< -6.3$ ) associated with both high  $(^{87}\text{Sr}/^{86}\text{Sr})_i$  ( $> 0.7137$ ) and  $(^{207}\text{Pb}/^{204}\text{Pb})_i$  ratios ( $> 15.68$ ) indicate that these metapelites were derived from the

erosion of an old crustal component and/or sediments.

## 6. Discussion

### 6.1. Main rock groups of the Raspas Metamorphic Complex

Field work, geochemical analyses and preliminary petrographic studies lead to distinguish three main rock groups within the Raspas Metamorphic Complex.



- Mafic HP metamorphic rocks include the eclogites and probably the serpentinised peridotites. Geochemical data indicate that these rocks likely represent remnants of a crustal section of an oceanic plateau (OPB) with the serpentinised peridotites corresponding to the residual part. No MORB-type rocks were found in this sample set.

- Metapelites, metamorphosed under HP conditions, were originally terrigenous sediments resulting from the erosion of an old continental crust. They are structurally associated with the eclogites and current petrographic studies suggest that both rock lithologies underwent comparable tectonic and  $P$ – $T$  evolutions.

- Epidote-bearing amphibolites were metamorphosed into greenschist to amphibolite facies (Río Panupali unit). These rocks display geochemical features indicating oceanic floor (MORB) affinities. No rocks with oceanic plateau characteristics occur in this unit.

Thus, the Raspas Metamorphic Complex exhibits a well defined internal structure, with independent tectono-metamorphic units, each one characterized by distinctive lithologies, metamorphic evolution and chemical affinities. This does not support the interpretation of a mere “tectonic mélange”. Since these tectono-metamorphic units are bounded by tectonic contacts, the present-day structural organization of the Raspas Metamorphic Complex is subsequent to the peak metamorphic conditions, and, therefore, results from its exhumation history. Additionally, this post-metamorphic tectonic evolution obscured the primary relationships between the distinct units and makes it difficult to propose a geodynamic evolution at this stage of the study.

## 6.2. Possible accretion processes

Because of their overthickened crust (15–40 km), oceanic plateaus are considered to be too buoyant to subduct and are more easily accreted or even obducted onto the continental margin (Ben Avraham et al., 1981; Cloos, 1993; Abbott et al., 1997). In the Raspas Metamorphic Complex, oceanic plateau basalts underwent eclogite facies metamorphism, indicating that part of the oceanic plateau can be subducted down to 40–60 km depth. However, we can reasonably consider that only a rather thin edge of the oceanic plateau, formed by basaltic flows and shallow level gabbroic

intrusions, has been subducted. When the thickest part of the oceanic plateau entered the subduction zone, it probably jammed the subduction and was accreted, thus leading to the westward jump or flip of the subduction zone.

The association of sediments of continental origin (metapelites) with remnants of oceanic plateau rocks (eclogites and peridotites), both metamorphosed under comparable high-pressure conditions, suggests that they underwent the same burial history. As the geochemical features of the metapelites clearly indicate that they were derived from the erosion of an old continental crust, they cannot constitute the submarine stratigraphic cover of the oceanic plateau. The subduction zone usually acts as a sediment trap that inhibits the bypass of products deriving from the continent onto the oceanic floor before the latter enters the subduction zone. On the other hand, the oceanic plateau is a submarine relief, on top of which no detrital sediments can be deposited, except—possibly—products of its own erosion.

Therefore, the continent derived metapelites were probably originally deposited at the foot of the Andean continental margin and structured as a classical sedimentary accretionary prism, such as those known in present-day accretionary margins (Von Huene and Scholl, 1991; Lallemand, 1999). As the edge of the oceanic plateau entered the subduction zone, it dragged down the accretionary wedge, which was buried along the Wadatti–Benioff zone, until the main body of the oceanic plateau jammed the subduction process.

In the Raspas Metamorphic Complex, rocks of N-MORB affinities metamorphosed under greenschist to amphibolite facies conditions are presently tectonically juxtaposed with oceanic plateau rocks showing HP assemblages. Such a tectonic framework seems to characterize the latest Jurassic–Early Cretaceous suture of northwestern South America. The Peltetec suture of the eastern Cordillera of Ecuador contains Jurassic lavas and greywackes of N-MORB and arc affinities, metamorphosed under greenschist facies during the latest Jurassic–Early Cretaceous (Litherland et al., 1994). In the suture zone of Colombia, most blueschist to amphibolite facies metamorphic rocks, dated between 129 and 110 Ma (Aspden and McCourt, 1986; Toussaint and Restrepo, 1994), are interpreted as remnants of oceanic plateau (Kerr et al., 1997).

If these two rock types had undergone the same geodynamic history, then we would expect an HP metamorphic overprint in the N-MORB rocks and a comparable or lower metamorphic grade in the oceanic plateau rocks, since the latter are theoretically less easily subducted than the former. This situation is not observed in the presently known outcrops ascribed to the latest Jurassic–Early Cretaceous suture. Therefore, the present-day Raspas–Peltetec–Colombian suture may represent a composite and/or polyphase feature involving at least two distinct large-scale tectono-metamorphic units, reflecting distinct geodynamic evolutions and significances.

### 6.3. Comparison with the northern Andes and Caribbean

Due to the northward component of the oceanic convergence in Late Cretaceous and Tertiary times (Pardo-Casas and Molnar, 1987) and to the evidences of large-scale dextral strike-slip movements of Tertiary age in northwestern South America (Freytmüller et al., 1993), remnants of Jurassic oceanic terranes, possibly equivalent to the Raspas mafic rocks, must be sought in the northern Andes and around the Caribbean plate.

In the suture zone of Colombia, remnants of oceanic plateau locally underwent HP metamorphism in the Early Cretaceous and, therefore, are of Jurassic age (Aspden and McCourt, 1986; Toussaint and Restrepo, 1994; Nivia, 1996; Kerr et al., 1997).

In Venezuela, the Siquisique ophiolites of Middle Jurassic age (Bartok et al., 1985) are considered petrologically comparable to the oceanic plateau assemblages of the Curaçao island (Donnelly et al., 1990), while Beets et al. (1984) postulate that the Margarita HP metabasic rocks (Sisson et al., 1997) are tholeiites of Late Jurassic age, possibly of MORB affinity. The Aptian–Albian La Rinconada unit (Margarita island, Venezuela) comprises HP gneisses and eclogites of MORB chemistry metamorphosed at ca. 500 °C and 12–14 kbar (Stockhert et al., 1995). The tectonic evolution of this complex requires a Pacific origin for the Caribbean plate. In the Lower Unit of the Santa Elena Peninsula (Costa Rica), Early Jurassic to Middle Cretaceous alkaline rocks (De Wever et al., 1985) exhibit OIB-like geochemical characteristics (Unit I, Hauff

et al., 2000) and are associated with an Early Cretaceous island arc suite (Astorga, 1997; Hauff et al., 2000).

In Hispaniola and Puerto Rico, pillow basalts are interbedded with ribbon radiolarian cherts of Late Jurassic–Early Cretaceous age and exhibit a Pacific affinity (Mattson and Pessagno, 1979; Montgomery et al., 1994). In Hispaniola and possibly in Puerto Rico, these MORB-type basalts probably emplaced near a hotspot (Donnelly et al., 1990; Lapierre et al., 1999).

The Raspas Metamorphic Complex may represent the southernmost outcrop of these Jurassic oceanic thickened crustal fragments scattered around the Cretaceous Caribbean Plate, since some of them present well documented oceanic plateau affinities or plume activity related signatures (Colombia, Costa Rica, Hispaniola).

## 7. Conclusions

- Geochemical and petrographic study of the Raspas Metamorphic Complex allowed us to identify several distinct litho-tectonic units: (1) HP mafic and ultramafic rocks with oceanic plateau affinities, (2) HP metapelites derived from an old continental crust, and (3) greenschist–amphibolite basalts and gabbros of N-MORB origin.

- Therefore, the Raspas Metamorphic Complex exhibits tectono-metamorphic units characterized by distinct lithologies, geochemical affinities and metamorphic conditions. Such a well defined internal structure does not support the interpretation of an accretionary wedge or a “tectonic mélange”.

- The evolution of the HP metamorphic rocks of the Raspas Metamorphic Complex may be explained by the dragging down of continent-derived sediments accumulated into an accretionary wedge as the edge of the oceanic plateau entered the subduction zone. Subsequently, the main body of the oceanic plateau stopped the subduction processes. Scattered Jurassic oceanic remnants, locally with plume-source affinity, known from northern South America and the Caribbean, may represent parts of this disrupted oceanic terrane.

- As for most Late Cretaceous–Paleogene accretions in Ecuador (Jaillard et al., 1997; Reynaud et al.,

1999), the accretion of the Raspas oceanic plateau occurred without obduction. In this model, underthrusting of parts of accreted oceanic terranes might contribute to the crustal thickening of the upper plate in this part of the Andes, as already suggested by Megard (1987, 1989) in Ecuador and further documented in Colombia by Weber et al. (2002).

• Along the latest Jurassic–Early Cretaceous suture of northwestern South America, oceanic plateau exhibit HP assemblages, whereas arc or N-MORB rocks show lower metamorphic grades. This suggests that this suture involves at least two distinct oceanic terranes characterized by distinct geodynamic evolution.

## Acknowledgements

This work was funded by a CNRS-INSU IT Programm, contribution no. 263, by the IRD, CSS1, and by the SNSF grant no. 20-50812.97. We would like to thank P. Telouk and the “Service Commun National du MC-ICPMS de l’Ecole Normale de Lyon”, as well as P. Brunet (UMR-5563), who carried out all the Sr–Nd TIMS analyses. The authors are grateful to M. Ballèvre (Univ. Rennes) and to G. Martinotti (Univ. Turin) for their invaluable help in petrographic study and field work, respectively. Luis Aguirre and Andrew Kerr are thanked for their constructive and helpful reviews of the manuscript.

## References

- Abbott, D.H., Drury, R., Mooney, W.D., 1997. Continents as lithological icebergs: the importance of buoyant lithospheric roots. *Earth Planet. Sci. Lett.* 149, 15–27.
- Arculus, R.J., Lapierre, H., Jaillard, E., 1999. A geochemical window into subduction–accretion processes: the Raspas Metamorphic Complex, Ecuador. *Geology* 27, 547–550.
- Aspden, J.A., McCourt, W.J., 1986. Mesozoic oceanic terrane in the Central Andes of Colombia. *Geology* 14, 415–418.
- Aspden, J.A., Bonilla, W., Duque, P., 1995. The El Oro metamorphic complex, Ecuador: geology and economic mineral deposits. *Overseas Geology and Mineral Resources*, vol. 67. British Geological Survey Publ., Nottingham, 63 pp.
- Astorga, A., 1997. El Puente istmo de América Central, y la evolución de la placa Caribe (con énfasis en el Mesozoico). *Profil* 12, 1–201, Stuttgart.
- Barrat, J.-A., Keller, F., Amossé, J., Taylor, R.N., Nesbitt, R.W., Hirata, T., 1996. Determination of rare earth elements in sixteen silicate reference samples by ICP-MS using a Tm addition and an ion-exchange chromatography procedure. *Geostand. Newsl.* 20, 133–139.
- Bartok, P.E., Renz, O., Westermann, G.E.E., 1985. The Siquisique ophiolites, northern Lara State, Venezuela; a discussion on their Middle Jurassic ammonites and tectonic implications. *Geol. Soc. Am. Bull.* 96, 1050–1055.
- Becker, H., Jochum, K.P., Carlson, R.W., 2000. Trace element fractionation during dehydration of eclogites from high-pressure terranes and the implications for element fluxes in subduction zones. *Chem. Geol.* 163, 65–99.
- Beets, D.J., Maresch, W.V., Klaver, G.T., Motana, A., Bocchio, R., Beunk, F.F., Monen, H.P., 1984. Magmatic rock series and high-pressure metamorphism as constraints on the tectonic history of the southern Caribbean. In: Bonini, W.E., et al. (Eds.), *The Caribbean–South American Plate Boundary and Regional Tectonics*. *Geol. Soc. Am. Mem.* 162, 95–130.
- Ben Avraham, Z., Nur, A., Jones, D., Cox, A., 1981. Continental accretion: from oceanic plateaus to allochthonous terranes. *Sciences* 213, 47–54.
- Ben Othman, D., White, W.M., Patchett, J., 1989. The geochemistry of marine sediments, island arc magma genesis and crust–mantle recycling. *Earth Planet. Sci. Lett.* 94, 1–21.
- Bourgeois, J., Toussaint, J.F., Gonzalez, H., Azema, J., Calle, B., Desmet, A., Murcia, L.A., Acevedo, A.P., Parra, E., Tournon, J., 1987. Geological history of the Cretaceous ophiolitic complexes of northwestern South America (Colombian Andes). *Tectonophysics* 143, 307–327.
- Brenan, J.M., Shaw, H.F., Phinney, D.L., Ryerson, F.J., 1994. Rutile–aqueous fluid partitioning of Nb, Ta, Hf, Zr, U and Th: implications for high field strength element depletions in island-arc basalts. *Earth Planet. Sci. Lett.* 128, 327–339.
- Cloos, M., 1993. Lithospheric buoyancy and collisional orogenesis: subduction of oceanic plateaus, continental margins, island arcs, spreading ridges, and seamounts. *Geol. Soc. Am. Bull.* 105, 715–737.
- Davidson, J.P., 1987. Crustal contamination versus subduction zone enrichment: examples from the Lesser Antilles and implications for mantle source compositions of island arc volcanic rocks. *Geochim. Cosmochim. Acta* 51, 2185–2198.
- De Wever, P., Azéma, J., Tournon, J., Desmet, A., 1985. Découverte de matériel océanique du Lias-Dogger inférieur dans la Péninsule de Santa Elena (Costa Rica, Amérique centrale). *C. R. Acad. Sci. Paris* 300, 759–764.
- Donnelly, T.W., Beets, D., Carr, M.J., Jackson, T., Klaver, G., Lewis, J., Maury, R., Schellekens, H., Smith, A.L., Wadge, G., Westercamp, D., 1990. History and tectonic setting of Caribbean magmatism. In: Dengo, G., Case, J.E. (Eds.), *The Caribbean Region, The Geology of Northern America*. *Geol. Soc. Am. Publ.*, vol. H, pp. 339–374.
- Duque, P., 1993. Petrology, metamorphic history and structure of El Oro Ophiolitic Complex, Ecuador. 2nd Internat. Symp. Andean Geodyn.-ISAG, Oxford 1993. *ORSTOM Publ.*, Paris, pp. 359–362.
- Feininger, T., 1980. Eclogite and related High-Pressure regional metamorphic rocks from the Andes of Ecuador. *J. Petrol.* 21, 107–140.

- Feininger, T., 1982. The metamorphic "basement" of Ecuador. *Geol. Soc. Am. Bull.* 93, 87–92.
- Feininger, T., Silberman, M.L., 1982. K–Ar geochronology of basement rocks on the Northern Flank of the Huancabamba deflection, Ecuador. *Open-File Rep.-U.S. Geol. Surv.*, 82–206, 21 pp.
- Freytmuller, J.T., Kellogg, J.N., Vega, V., 1993. Plate motions in the North Andean region. *J. Geophys. Res.* 98, 21853–21863.
- Gabriele, P., Ballèvre, M., Jaillard, E., Hernandez, J., 1999. Decompression at decreasing temperatures in eclogite-facies metapelites (El Oro metamorphic complex, SW-Ecuador): a record of fast exhumation rates. 4th Internat. Symp. Andean Geodyn.-ISAG, Göttingen 1999. *IRD Publ.*, Paris, pp. 245–248.
- Hart, S.R., 1984. A large-scale isotope anomaly in the southern hemisphere mantle. *Nature* 309, 753–757.
- Hart, S.R., Gerlach, D.C., White, W.M., 1986. A possible new Sr–Nd–Pb mantle array and consequences for mantle mixing. *Geochim. Cosmochim. Acta* 50, 1551–1557.
- Hauff, F., Hoernle, K., van den Bogaard, P., Alvarado, G., Garbe-Schönberg, D., 2000. Age and geochemistry of basaltic complexes in western Costa Rica: contributions to the geotectonic evolution of Central America. *Geochem. Geophys. Geosyst.* 1 1999-GC-000020.
- Hoernle, K.A., Tilton, G.R., 1991. Sr–Nd–Pb isotope data for Fuerteventura (Canary Islands) basal complex and subaerial volcanics: applications to magma genesis and evolution. *Schweiz. Mineral. Petrogr. Mitt.* 71, 3–18.
- Hofmann, A.W., Jochum, K.P., Seufert, M., White, W.M., 1986. Nb and Pb in oceanic basalts: new constraints on mantle evolution. *Earth Planet. Sci. Lett.* 79, 33–45.
- Hughes, R.A., Pilatasig, L.F., 2002. Cretaceous and Tertiary terrane accretion in the Cordillera Occidental of the Andes of Ecuador. *Tectonophysics* 345, 29–48.
- Jaillard, E., Benitez, S., Mascle, G.H., 1997. Les déformations de la zone d'avant-arc sud-équatorienne en relation avec l'évolution géodynamique. *Bull. Soc. Geol. Fr.* 168, 403–412.
- Kerr, A.C., Tarney, J., Marriner, G.F., Klavere, G.T., Saunders, A.D., Thirlwall, M.F., 1996. The geochemistry and petrogenesis of the late Cretaceous picrites and basalts of Curaçao, Netherlands Antilles: remnant of an oceanic plateau. *Contrib. Mineral. Petrol.* 124, 29–43.
- Kerr, A.C., Marriner, G.F., Tarney, J., Nivia, A., Saunders, A.D., Thirlwall, M.F., Sinton, C.W., 1997. Cretaceous basaltic terranes in Western Colombia: elemental, chronological and Sr–Nd isotopic constraints on petrogenesis. *J. Petrol.* 38, 677–702.
- Kretz, R., 1983. Symbols for rock-forming minerals. *Am. Mineral.* 68, 276–279.
- Lallemant, S., 1999. *La Subduction Océanique*. Gordon & Breach, Amsterdam, 194 pp.
- Lapierre, H., Dupuis, V., Mercier de Lépinay, B., Tardy, M., Ruiz, J., Maury, R.C., Hernandez, J., Loubet, M., 1997. Is the Lower Duarte Igneous Complex (Hispaniola) a remnant of the Caribbean plume-generated oceanic plateau? *J. Geol.* 105, 111–120.
- Lapierre, H., Dupuis, V., Mercier de Lépinay, B., Bosch, D., Monié, P., Tardy, M., Maury, R.C., Hernandez, J., Polvé, M., Yeghicheyan, D., Cotten, J., 1999. Late Jurassic oceanic crust and Upper Cretaceous Caribbean Plateau picritic basalts exposed in the Duarte Igneous Complex. *J. Geol.* 107, 193–207.
- Lapierre, H., Bosch, D., Dupuis, V., Polvé, M., Maury, R.C., Hernandez, J., Monié, P., Yeghicheyan, D., Jaillard, E., Tardy, M., Mercier de Lépinay, B., Desmet, A., Keller, F., Senebier, F., 2000. Multiple plume events in the genesis of the peri-Caribbean Cretaceous oceanic plateau province. *J. Geophys. Res.* 105 (B4), 8403–8421.
- Litherland, M., Aspden, J.A., Jemielita, R.A., 1994. The metamorphic belts of Ecuador. *Brit. Geol. Surv., Overseas Mem.*, 11, 147 p., 2 maps, Keyworth, UK.
- Lucassen, F., Franz, G., Laber, A., 1999. Permian High Pressure rocks; the basement of the Sierra de Limón Verde in northern Chile. *J. South Am. Earth Sci.* 12, 183–199.
- Mahoney, J.J., Natland, J.H., White, W.M., Podera, R., Bloomer, S.H., Fisher, R.L., Baxter, A.N., 1989. Isotopic and geochemical provinces of the western Indian ocean spreading centers. *J. Geophys. Res.* 94, 4033–4052.
- Malfere, J.L., Bosch, D., Lapierre, H., Jaillard, E., Arculus, R., Monié, P., 1999. The Raspas Metamorphic Complex (Southern Ecuador): remnant of a late Jurassic–early Cretaceous accretionary prism. Part II: geochemical and isotopic constraints. 4th Internat. Symp. Andean Geodyn.-ISAG, Göttingen. *IRD Publ.*, Paris, pp. 245–248.
- Manhès, G., Allègre, C.J., Dupré, B., Hamelin, B., 1978. Lead–lead systematics, the age and chemical evolution of the Earth in a new representation space. *Earth Planet. Sci. Lett.* 44, 91–104.
- Mattson, P.H., Pessagno, J.E.A., 1979. Jurassic and Early Cretaceous radiolarians in Puerto Rican ophiolite: tectonic implications. *Geology* 7, 440–444.
- Mégar, F., 1987. Cordilleran and marginal Andes: a review of Andean geology North of Africa elbow (18°S). In: Monger, J.W.H., Francheteau, J. (Eds.), *Circum-Pacific Orogenic Belts and Evolution of the Pacific Ocean Basin*. American Geophysical Union, Geodynamic Series, vol. 18, pp. 71–95.
- Mégar, F., 1989. The evolution of the Pacific Ocean margin in South America North of Africa elbow (18°S). In: Ben Avraham, Z. (Ed.), *The Evolution of the Pacific Ocean Margin*, Oxford. *Monogr. Geol. Geophys.*, vol. 8. Oxford Univ. Press, New York, pp. 208–230.
- Montgomery, H., Pessagno Jr., E.A., Lewis, J.F., Schellekens, J., 1994. Paleogeography of Jurassic fragments in the Caribbean. *Tectonics* 13, 725–732.
- Mourier, T., Laj, C., Mégar, F., Roperch, P., Mitouard, P., Farfan-Medrano, A., 1988. An accreted continental terrane in Northwestern Peru. *Earth Planet. Sci. Lett.* 88, 182–192.
- Newson, H.E., White, W.M., Jochum, K.P., Hofmann, A.W., 1986. Siderophile and chalcophile element abundances in oceanic basalts, Pb isotope evolution and growth of the Earth's core. *Earth Planet. Sci. Lett.* 80, 299–313.
- Nivia, A., 1996. The Bolivar mafic–ultramafic complex, SW Colombia: the base of an obducted oceanic plateau. *J. South Am. Earth Sci.* 9, 59–68.
- Pardo-Casas, F., Molnar, P., 1987. Relative motion of the Nazca (Farallón) and South America plate since late Cretaceous times. *Tectonics* 6, 233–248.
- Reynaud, C., Jaillard, E., Lapierre, H., Mamberti, M., Mascle, G.H.,

1999. Oceanic plateau and island arcs of Southwestern Ecuador: their place in the geodynamic evolution of northwestern South America. *Tectonophysics* 307, 235–254.
- Sisson, V.B., Ertan, I.E., Avé Lallemand, H.G., 1997. High Pressure ( $\approx 2000$  MPa) kyanite- and glaucophane-bearing pelitic schist and eclogite from Cordillera de la Costa Belt, Venezuela. *J. Petrol.* 38, 65–83.
- Snow, J.E., Hart, S.R., Dick, H.J.B., 1994. Nd and Sr isotope evidence linking mid-ocean-ridge basalts and abyssal peridotites. *Nature* 371, 57–60.
- Staudigel, H., Park, K.H., Pringle, M., Rubenstone, J.L., Smith, W.H.F., Zindler, A., 1991. The longevity of the South Pacific isotopic and thermal anomaly. *Earth Planet. Sci. Lett.* 102, 24–44.
- Stille, P., Unruh, D.M., Tatsumoto, M., 1986. Pb, Sr, Nd and Hf isotopic constraints on the origin of Hawaiian basalts and evidence for a unique mantle source. *Geochim. Cosmochim. Acta* 50, 2303–2320.
- Stockhert, B., Maresch, W.V., Brix, M., Kaiser, C., Toetz, A., Kluge, R., Kruckhans-Lueder, G., 1995. Crustal history of Margarita island (Venezuela) in detail: constraints on the Caribbean plate-tectonic scenario. *Geology* 23, 187–190.
- Sun, S.S., McDonough, W.F., 1989. Chemical and Isotopic Systematics of Oceanic Basalts; Implications for Mantle Composition and Processes. *Geol. Soc. Spec. Publ.*, vol 42, 313–345.
- Taylor, S.R., McLennan, S.M., 1985. The continental crust: its composition and evolution. An Examination of the Geochemical Record Preserved in Sedimentary Rocks. Blackwell, Oxford, 312 pp.
- Toussaint, J.-F., Restrepo, J.J., 1994. The Colombian Andes during Cretaceous times. In: Salfity, J.A. (Ed.), *Cretaceous Tectonics in the Andes*. Earth Evolution Sciences Vieweg, Braunschweig, pp. 61–100.
- Vidal, P., Chauvel, C., Brousse, R., 1984. Large mantle heterogeneity beneath French Polynesia. *Nature* 307, 536–538.
- Von Huene, R., Scholl, D.W., 1991. Observations at convergent margins concerning sediment subduction, subduction erosion, and the growth of continental crust. *Rev. Geophys.* 29, 279–316.
- Wasserburg, G.J., Jacobsen, S.B., DePaolo, D.J., McCulloch, M.T., Wen, T., 1981. Precise determination of Sm/Nd ratios, Sm and Nd isotopic abundance in standard solutions. *Geochim. Cosmochim. Acta* 45, 2311–2323.
- Weber, M.B.I., Tarney, J., Kempton, P.D., Raymond, R.W., 2002. Crustal make-up of the Northern Andes: evidence based on deep crustal xenolith suites, Mercaderes, SW Colombia. *Tectonophysics* 345, 49–82.
- White, W.M., Hofmann, A.W., Puchelt, H., 1987. Isotope geochemistry of Pacific mid-ocean ridge basalt. *J. Geophys. Res.* 92, 4881–4893.
- White, W.M., McBirney, A.R., Duncan, R.A., 1993. Petrology and geochemistry of the Galapagos Islands: portrait of a pathological mantle plume. *J. Geophys. Res.* 98, 19533–19563.